**JAST**. Vol. 9, No. 2, pp 59-70


JAST
Journal of Aerospace Science and Technology

# Parametric Study of the Empty and Foam-Filled End-Capped Conical Tubes under Quasi Static and Dynamic Impact Loads

A. Ghamarian[1], H.R. Zarei[2]

*This paper investigates the parametric study of the empty and foam-filled end-capped tubes under quasi static and dynamic loadings. The numerical crash analysis of the empty and foam-filled tubes was performed using the explicit finite element code ABAQUS- explicit. Satisfactory agreements were generally achieved between the numerical and experimental results. In order to determine the crash behavior of the empty and foam filled tubes under dynamic impact, the dynamic amplification factor which related the quasi-static results to dynamic responses was determined. The influence of the various parameters on the dynamic responses was investigated and then compared with the quasi-static results.*

***Keywords**: End-Capped Conical Tubes, Dynamic Impact.*

## 1 Introduction

There has been considerable activity on dynamic crush of thin-walled aluminum tubes during the past decade. A significant part of this effort has been concerned with the use of these structures in energy absorbing systems. Several researchers studied the crash response of aluminum tubes with different cross sections geometries and in several points of view; namely, analytical, numerical and experimental. Wierzbicki and Abramowicz [1] presented a simple formula to predict the axial crash response of thin-walled columns. Their method is based on the balance of external and internal work. This model was validated experimentally by Abramowizc and Jones [2]. Alexander [3], Pugsley [4], Abramowicz [5] and Abramowicz and Jones [6], Singace and Elsobky [7] and Wierzbicki and Bhat [8] also used the same method to predict the crash behavior of circular tubes. Some researchers used crashworthiness optimization technique to find optimum aluminum tubes which have maximum energy absorption capacity [9, 10].

According to the previous investigations, thin-walled conical tubes under crushing load achieve different crushing modes based on their length and cross section dimensions. They collapse either in axisymmetric mode (concertina or ring mode) or non axisymmetric mode (diamond mode) or mixed mode [11]. Energy absorption normally takes place by progressive buckling of tubes walls. A distinctive feature of such a deformation mechanism is that the rate of energy dissipation is concentrated over relatively narrow zones.

Prasad and Gupta [12] performed some crush experiments on conical frusta samples with large semi-apex angles at various strain rates. Numerical and experimental studies were carried out by Gupta et al. [13] to explore the influence of rolling and stationary plastic hinges in the post-buckling pattern of quasi statically loaded conical tubes. They finally compared their experimental and numerical results. Gupta and Venkatesh [14] reported experimental studies on the performance of conical frusta subjected to quasi-static and dynamic axial crush loadings.

*1. Astronautics Research Institute, Iranian Space Research Center, 14665-834, Tehran, Iran.*

*2. Aeronautical University of Science and Technology, Tehran, Iran. Email: hrzmo2000@yahoo.com*

Cellular solids are increasingly used in many engineering applications like energy absorption, thermal insulation and lightweight structures due to their unique property of high porosity. These materials show a distinct plateau of almost constant stress under compressive uniaxial load with the nominal strain value up to 80% [15], which indicates high energy absorption capacity. For light weight energy absorber designs, low density metal fillers, such as aluminum honeycomb or foam, are preferred to tube with thicker tube walls in terms of achieving the same energy absorption. Metal fillers are able to increase the energy absorption of a thin-walled column. This increase is the result of the large compressive deformation of the filler. The investigations indicated that the interaction between the filler and the tube walls increase the energy absorption capacity of the filled tubes. The mean crushing loads of the filled tubes are found to be higher than the sum of the crushing loads of foam alone and tube alone.

Although several researches have been conducted to study the crush response of foam-filled rectangular and circular tubes [16-19], relatively few studies have focused on the energy absorption performance of foam-filled conical tubes. Some useful experimental and numerical investigations were carried out to establish the load-deflection and collapse mode responses of the foam-filled conical tubes [20]. Gupta and Velmurugan experimentally found that the energy absorption capacity of foam filled conical composite tube is significantly higher than an empty one. More recently, the crushing response of empty and foam-filled conical members under axial impact loading was investigated [21-23].

The end-capped conical tubes are applied in the nose of sounding rocket as both a cover and an energy absorber. Recently, the energy absorption mechanisms of the end-capped circular and conical tubes as well as circular tubes with shallow spherical caps were investigated [24-26]. The present research is concerned with the response of end-capped conical tubes under axial compressive load in order to determine the effects of the end cap on the crushing mechanism, crushing load and energy absorption capacity. Several quasi static crash experiments are carried out on empty and foam-filled end-capped conical tubes. A finite element model, which is validated using existing experimental results, is used to perform the parametric study. The model is also used to determine dynamic amplification factor so as to quantify the effect of various parameters on the dynamic response of the tubes. The results demonstrate the advantages of the end-capped conical tubes with a noticeable improvement in the initial peak load and decrease in the deceleration pulse.

## 2 Experimental test program

The end-capped conical tubes were fabricated from aluminum plates through spinning process. The circular blanks were cut from commercial aluminum plates with thickness of 1 mm and were stretched over the surface of a rotating die. The end-capped thickness of conical tubes is the same as the blank thickness; however, there is some thickness gradient on conical wall due to stretching the blanks over the die surface. The edge of the formed tubes on the open side was trimmed by moving the cutting tool normal to the rotation axis of the sample at the end of forming process. Some samples were filled with polyurethane foam which is composed of two components called base and accelerator. The average geometries of the empty and foam-filled end-capped conical tubes are shown in Table 1 with the following identification system. Here ‘‘C’’ and ‘‘FC’’ signify the empty and polyurethane filled end-capped conical tube, respectively. The main geometric parameters are: the tube wall thickness t, length L, top end diameter $D_1$ and bottom end diameter $D_2$. The specimens obtained from the process of spinning were found to have a variation in their thicknesses along the meridian direction. Their thicknesses were found to be maximum $t_1$, at the smaller end and minimum $t_2$, at the larger end; while the variation is almost linear [24,27].

The elastic and plastic behaviors of aluminum materials were determined using tensile testing of the coupons cut from plates. Fig. 1a shows the true stress-plastic strain curve for aluminum material. The elastic modulus, Poisson’s ratio and initial yield stress of aluminum material were determined as 55.7 GPa, 0.3 and 83.3 MPa, respectively. Uniaxial compression tests were performed on the square cubes of polyurethane foams to determine the material parameters at large deformation. The dimension of square cubes was 50 mm and the test was performed in accordance with ASTM D1621–04 standard. As shown in Fig. 1b, stress-strain curves

**Table 1. The geometrical dimensions of empty and foam filled end-capped conical tubes**

| Sample type | Density $\rho_f$ (kg/m$^3$) | Height h (mm) | Top Diameter $D_1$(mm) | Bottom Diameter $D_2$ (mm) | Thickness | |
|---|---|---|---|---|---|---|
| | | | | | $t_1$ (mm) | $t_2$ (mm) |
| $C_1$ | 0 | 97.5 | 31.1 | 65.1 | 1.0 | 0.85 |
| $C_2$ | 0 | 97.5 | 31.4 | 65.2 | 1.0 | 0.84 |
| $C_3$ | 0 | 96.9 | 31.2 | 65.4 | 1.0 | 0.83 |
| $C_4$ | 0 | 97.8 | 31.1 | 65.2 | 1.0 | 0.85 |
| $FC_1$ | 65 | 97.3 | 31.1 | 65.1 | 1.0 | 0.86 |
| $FC_2$ | 65 | 97.5 | 31.2 | 65.3 | 1.0 | 0.83 |
| $FC_3$ | 90 | 97.5 | 31.1 | 65.2 | 1.0 | 0.85 |
| $FC_4$ | 90 | 97.7 | 31.3 | 65.1 | 1.0 | 0.84 |
| $FC_5$ | 145 | 97.4 | 31.1 | 65.1 | 1.0 | 0.84 |
| $FC_6$ | 145 | 97.6 | 31.4 | 65.3 | 1.0 | 0.86 |

of the polyurethane foams illustrate an initial elastic behavior followed by a plateau region in which there is less variation in stress as the strain increases. Finally, the stress rapidly increases with further strain in the densification region due to high reduction of void content in porous polyurethane foams.

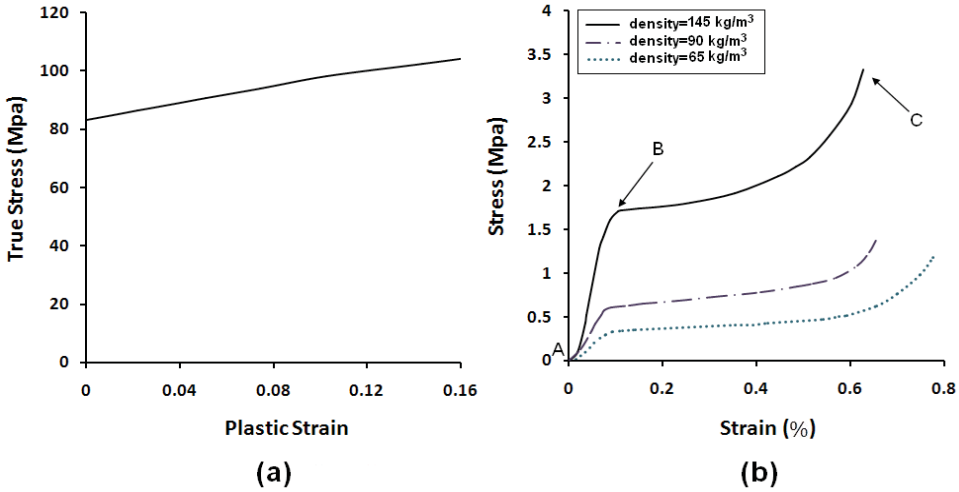


**Figure 1. Typical stress-strain curves for (a) aluminum material and (b) polyurethane foams [24].**

Quasi-static crash tests were carried out in a 60-ton universal testing machine. The experimental setup is shown in Fig. 2a. The load was applied through a thick steel plate contacting the cap of conical tube. Tests were carried out on empty and polyurethane foam-filled conical tubes at a constant crosshead speed of 10 mm/min. The specimen was fixed at the open edge of the tubes inside the circular hole of the part attached to the fixed table of testing machine, as shown in Fig. 2b. The height of circular hole is 3 mm and its diameter matches the outside diameter of tubes. Fig. 3 shows the deformed geometries of the specimens. The geometric analysis of specimens revealed that there are low amplitude imperfections in conical tube. Therefore, the conical tubes were buckled in axisymmetric deformation mode. The force and displacement of the crosshead were measured during axial compression and the results were used to determine initial peak load, average load and energy absorption capacity of the empty and foam-filled end-capped conical tubes.

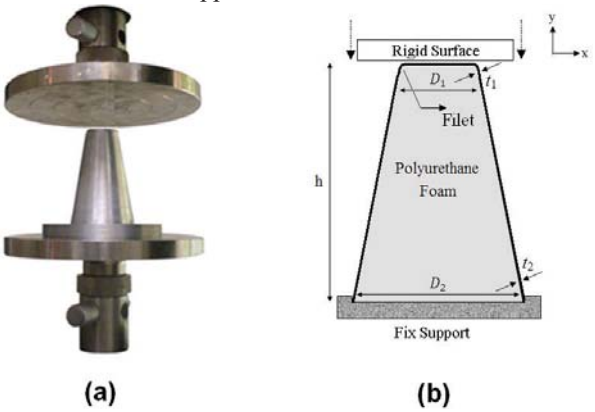


**Figure 2. (a) Experimental setup and (b) the schematics of specimen and fixture for crushing test.**

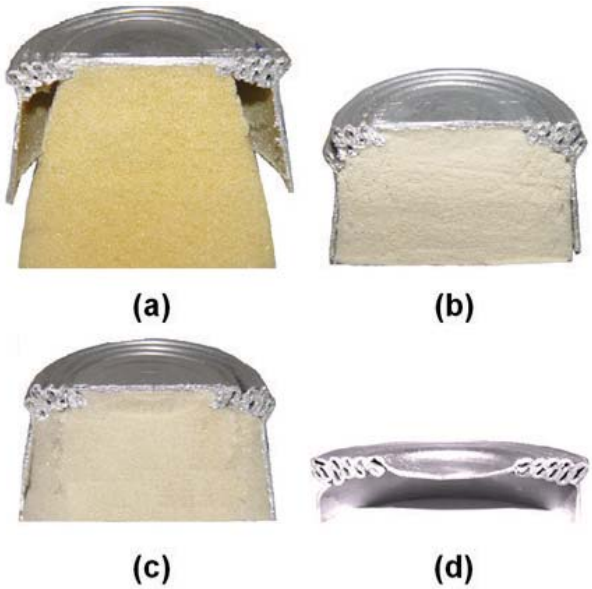


**Figure 3. Photographic views of the deformed geometry for: (a) $FC_5$ (b) $FC_3$ (c) $FC_1$ and (d) $C_1$.**

The load-displacement curves of the empty and foam-filled end-capped conical tubes are shown in Fig.4. It can be observed that the curves are fluctuating in a wavy shape. The curves of the empty and foam-filled end-capped conical tubes are similar. Here, it can be seen that for every foam density, the first peak of the foam-filled conical tube is higher than that the first peak of the empty one. In this case, the presence of the sta-

tionary as well as the rolling plastic hinge for the empty and filled tubes can be recognized. The number of the peaks is corresponding to the number of lobes in deformed specimens. An important observation is that the load-displacement curve of polyurethane foam-filled conical tubes with higher density tends to lie above the conical tubes filled with lower foam density and empty conical tube. This is because the foam constrains the localized buckling of the conical tube wall and more energy is required to bend them. The results obtained from the quasi static compression tests on foam-filled conical tubes are shown in Table 2.

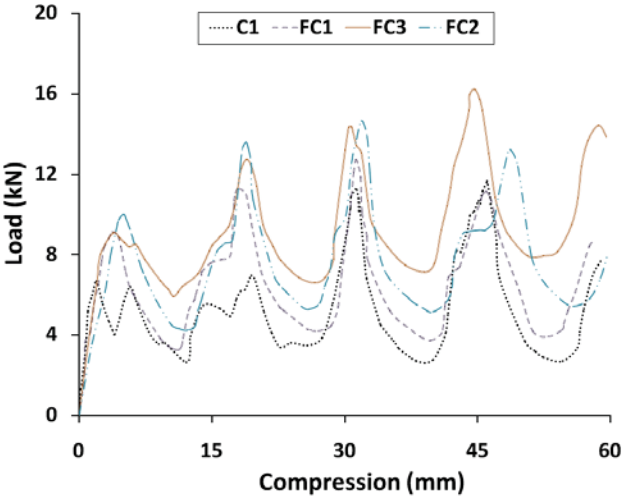


**Figure 4. Quasi-static load-deflection curves of the empty and foam-filled conical tubes with different polyurethane foam densities**

**Table 2. Results from quasi-static tests conducted on empty and foam-filled conical tubes for 60 mm compression**

| Sample type | Foam density $\rho_f$ (kg/m$^3$) | Initial peak load $F_i$ (kN) | Energy absorption $E_a$ (J) | Specific energy $E_s$ (J/gr) | Average load $F_{ave}$ (kN) | Load ratio $\eta$ (-) |
|---|---|---|---|---|---|---|
| $C_1$ | 0 | 6.7 | 318 | 15.50 | 5.30 | 0.79 |
| $C_2$ | 0 | 6.5 | 312 | 15.63 | 5.20 | 0.80 |
| $C_3$ | 0 | 6.8 | 308 | 15.02 | 5.13 | 0.75 |
| $C_4$ | 0 | 6.6 | 324 | 15.69 | 5.40 | 0.81 |
| $FC_1$ | 65 | 9.4 | 378 | 12.55 | 7.01 | 0.74 |
| $FC_2$ | 65 | 9.2 | 371 | 12.05 | 6.18 | 0.67 |
| $FC_3$ | 90 | 10.1 | 450 | 12.04 | 8.29 | 0.82 |
| $FC_4$ | 90 | 10.3 | 461 | 12.23 | 7.68 | 0.75 |
| $FC_5$ | 145 | 9.1 | 553 | 13.88 | 9.22 | 1.01 |
| $FC_6$ | 145 | 9.1 | 559 | 13.98 | 9.32 | 1.02 |

## 3 Numerical simulation

A finite element model was developed to analyze the axial quasi-static and dynamic crushing responses of empty and foam-filled conical tubes. The ABAQUS explicit finite element code was used to carry out the simulations [28]. The numerical model was able to simulate the buckling and post-buckling problems considering the material and geometric non-linearity. Based on the experimental observations, an axisymmetric condition was considered to model the large deformation of conical tubes. Fig. 5 illustrates geometric modeling which consists of three parts including (1) specimen, (2) fixed rigid body, and (3) moving rigid body. A specific mass was assigned to the moving rigid body to simulate the mass of the impacting device. It was assumed that there was no initial imperfection in the conical tubes and the wall thickness varied linearly between close and open edges.

The geometries of thin-wall tube and foam material were meshed by four-node axisymmetric continuum elements, which were suitable for large plastic deformation [29]. To find the adequate element size, a sensitivity analysis was carried out to obtain accurate results within a reasonable computational time. The fixed and moving bodies were assumed to be rigid compared to the specimen and were meshed using two-node axisymmetric rigid elements.

The axial compression was simulated by applying a constant velocity to the upper rigid surface along y-axis, as shown in Fig. 5. Contact boundary condition was considered between the moving rigid surface and the upper surface of the end-capped specimen. To prevent penetration from the wrinkled surfaces of the tube wall during progressive buckling, self-contact conditions were considered on the internal and external surfaces of tube wall. The lower rigid surface was constrained to the ground. The contact boundary conditions were also considered between the boundary surface of foam material and inner surfaces of the tube and lower rigid surface. The coefficient of friction was set to 0.15 in the contact surfaces. The nodes located at the bottom of the tube were tied to the fixed rigid surface for the purpose of modeling the clamped-end constraint.

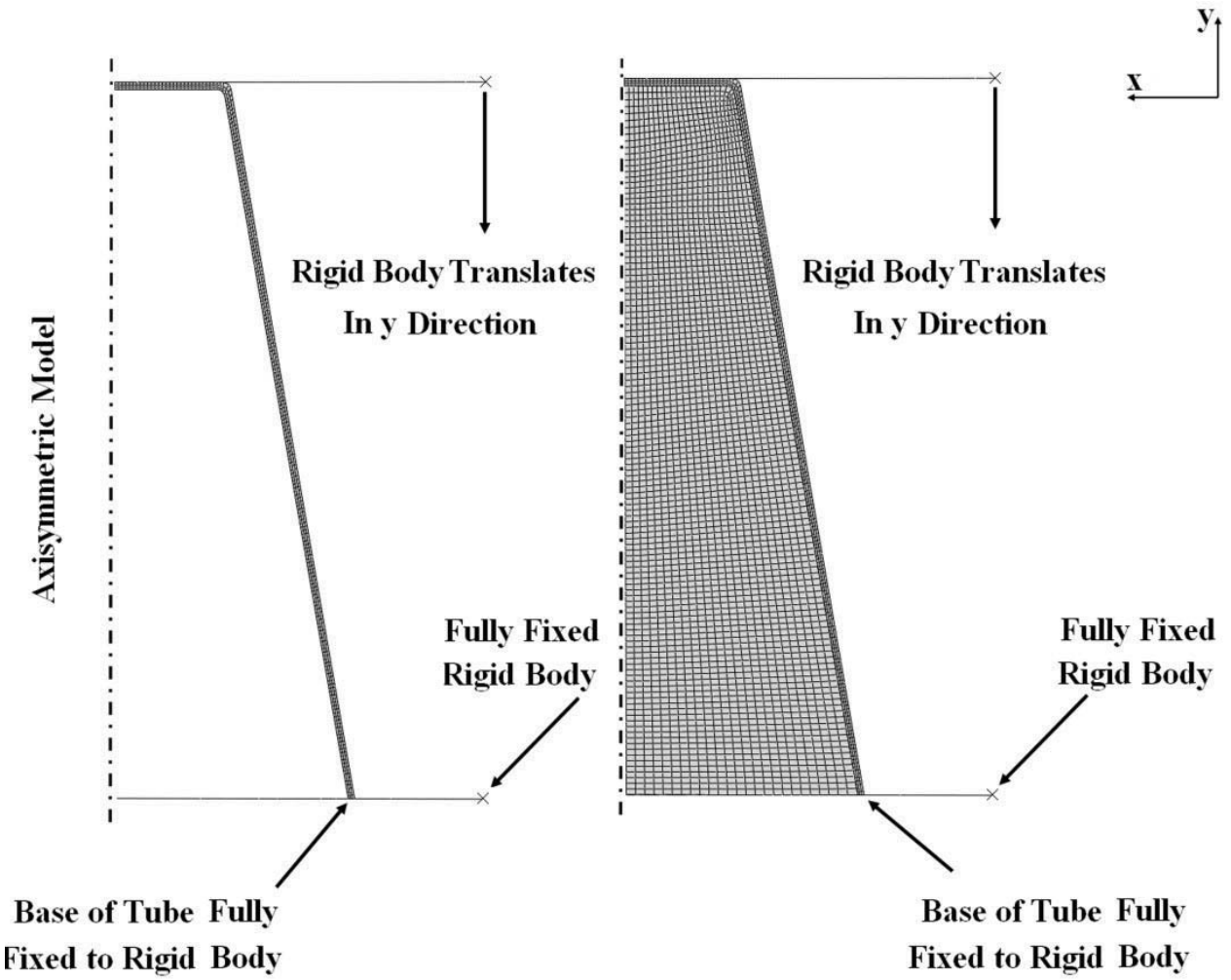


**Figure 5. Axisymmetric geometric modeling for: (a) empty and (b) foam-filled conical tubes.**

The mechanical response of aluminum tubes was characterized using elastoplastic model. The plastic behavior was described by engineering stress and strain measured in uniaxial tensile test, which are denoted here by $\sigma_E$ and $\varepsilon_E$, respectively. Such measurements were converted to true stress and plastic strain as follows:

$$\sigma_T = \sigma_E(1+\varepsilon_E) \tag{1}$$

$$\varepsilon_p = Ln(1+\varepsilon_E) - \frac{\sigma_T}{E} \tag{2}$$

where $\sigma_T$ and $\varepsilon_p$ are true stress and plastic strain, respectively. The approximate true stress and plastic strain data used as the input value for finite element models are listed in Table 3.

**Table 3. True stress-plastic strain for aluminum material of conical tubes [24]**

| $\sigma_T$ (MPa) | 83.3 | 90.6 | 94.0 | 98.2 | 102.4 | 104.1 |
|---|---|---|---|---|---|---|
| $\varepsilon_P$ | 0 | 0.051 | 0.074 | 0.103 | 0.143 | 0.154 |

The mechanical response of polyurethane foam was described by crushable foam material model developed by Deshpande and Fleck [30]. Table 4 lists the material parameters for polyurethane foam based on the crushable foam model. The elastic modulus of polyurethane foam was determined using the slope of line A–B, shown in Fig. 1. The Poisson's ratio in elastic (v) and plastic ($v_p$) region was assumed to be zero. The initial yield stress in uniaxial compression is the stress value at point B as shown in Fig. 1 and yield stress during the deformation was determined based on the experimental data corresponding to the curve between points B and C. The yield stress ratio (k) was set to a unit value [24]. The hardening law defines the value of the yield stress in uniaxial compression as a function of the absolute value of axial plastic strain. Table 4 tabulates the foam parameters used in this study.

**Table4. Tabulated crushable foam mechanical properties used in simulation [24]**

| Density (kg/m$^3$) | Elasticity | | Plasticity | |
|---|---|---|---|---|
| | E(MPa) | υ | k | $v_p$ |
| 65 | 5.5 | 0 | 1 | 0 |
| 90 | 10.9 | 0 | 1 | 0 |
| 145 | 27.2 | 0 | 1 | 0 |

The yield stress in dynamic loading is dependent on plastic strain rate. The empirical power law developed by Cowper-Symonds [31] is used to consider the effect of plastic strain rate on yield stress of both aluminum and foam materials, as follows:

$$\dot{\varepsilon}_p = D\left(\frac{\sigma_d}{\sigma_s} - 1\right)^m \quad (3)$$

where $\sigma_s$ and $\sigma_d$ denote the quasi-static and dynamic yield stresses, respectively, and D and *m* are material constants [32-33].

## 4 Model verification

The calculated response parameters from the FE models are:

1. Crushing length (X), which is the length of deformed tubes
2. The initial peak crush load ($F_i$)
3. The mean crush load ($F_{ave}$), that is defined as the load calculated for a reduction in tube length
4. Specific absorbed energy ($E_a$), which is the energy absorbed by the tube divided by the total mass of the tube
5. Load ratio or performance of the tube (η), which is defined as the ratio of the mean crush load. To ensure that the FE model was sufficiently accurate, it was validated against the experimental data. The final crushed shape of the end-capped empty and foam-filled conical tubes are shown in Fig.6 and compared with the experimental observation.

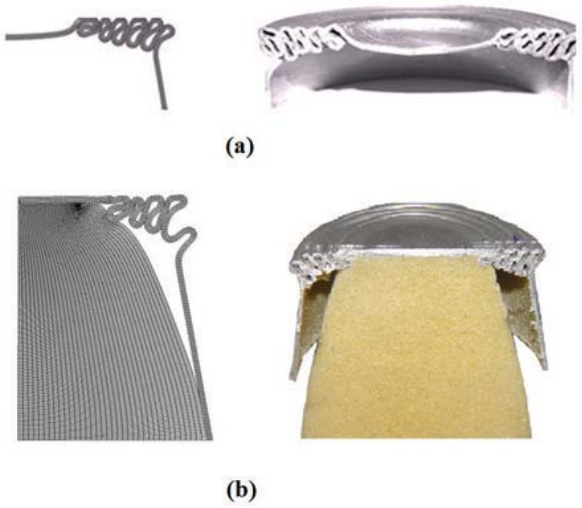


**Figure 6. Comparison of collapse modes of (a) empty and (b) filled conical tubes with density of 145 kg/m3 from the numerical and experimental results.**

Experimental and numerical crash load-deformation curves are plotted in Fig.7. It is observed that the numerical values are close to the experiments. The first peaks correspond to the initial collapse when the conical tube behaves elastically. The separation of the end-capped surface from upper rigid surface leads to forming the first fold at the fillet region. The outward radial motion of the first fold is possible up to a limited value and then the next fold is generated, while it is moved toward the inside of tube. Such folds act as imperfection causing the next folds to be generated adjacent to the previous folds. It can be seen that the crash force is fluctuated around a mean value of the axial force.

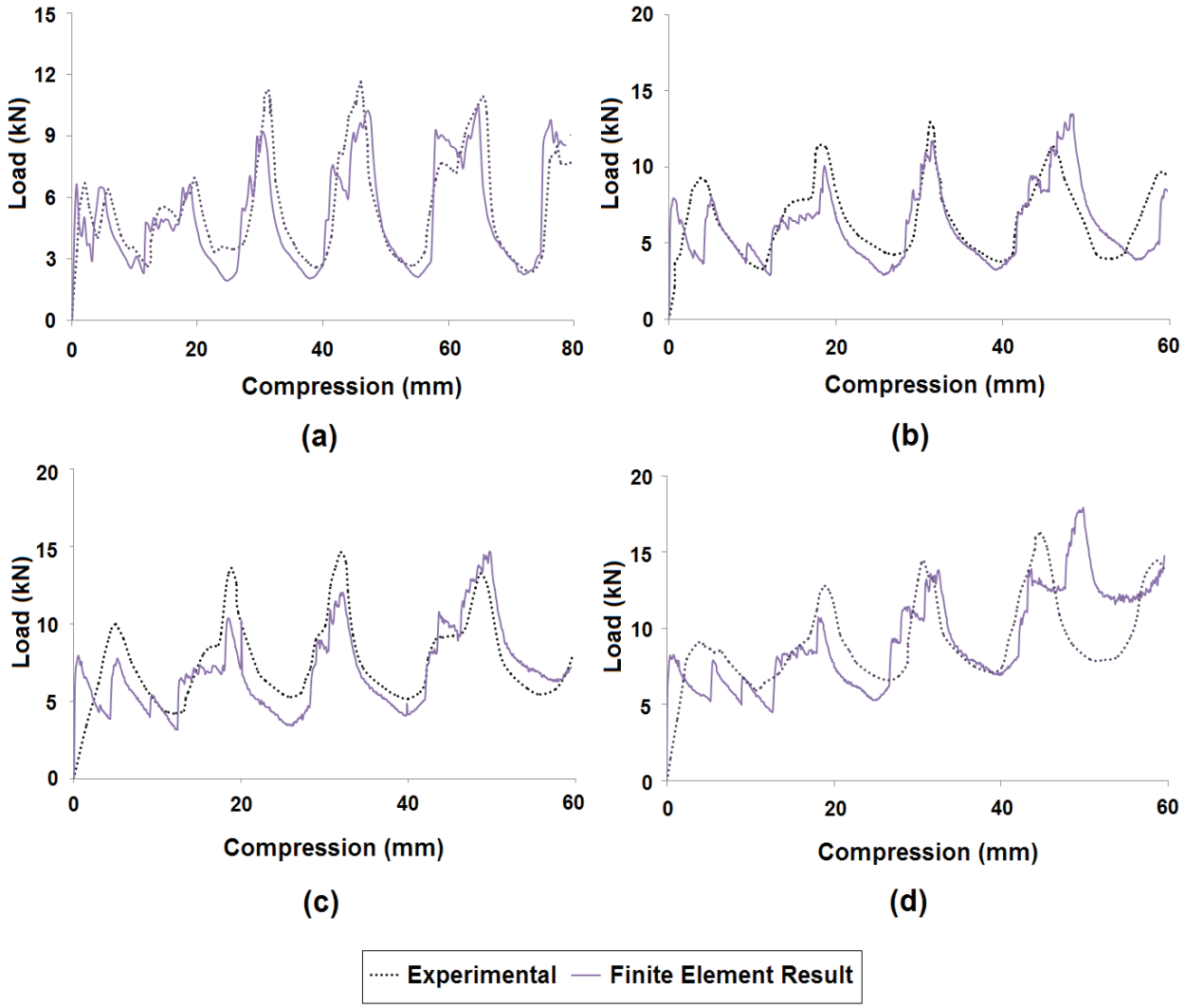


**Figure 7. Comparison of experimental and numerical static load-displacement curves for (a) $C_1$, (b) $FC_1$, (c) $FC_3$, and (d) $FC_5$**

## 5 Dynamic loading

The explicit finite element method was used to analyze the dynamic response of the empty and foam-filled end-capped conical tubes subjected to axial impact loading. The effect of strain rate on the yield stress is described by Eq. (3), the parameters of which are listed in Table 5 for both aluminum and foam materials. The numerical model was used to calculate the energy absorption capacities of the conical end-capped tubes under different impact velocities. It was also of the interest to quantify the effect of the various parameters of the tubes on the dynamic responses and then compare them with the quasi-static response, using the Dynamic Amplification Factor (DAF). This factor is important in a simple design procedure as it can be used to estimate the dynamic effect from the static analyses without conducting actual dynamic analyses or tests. In the present study, the DAF represented the ratio of energy absorbed under dynamic loading to the energy absorbed under quasi static loading for the various impact velocities and foam densities with a constant impact mass. In this section, the DAF of the empty conical tube was compared with conical tube filled with a foam density of 145 Kg/m$^3$ for varying wall thickness, semi-apical angle and impact velocity.

**Table 5. Parameters describing the strain rate effect on yield stress of aluminum and polyurethane foam materials [24,34]**

| Material | $D\ (s^{-1})$ | $m$ |
|---|---|---|
| Aluminum | 1288000 | 4 |
| Polyurethane foam | 4638 | 2.285 |

### 5.1 Effect of impact velocity on the DAF

Fig. 8 illustarets the effect of impact velocity on the DAF of the absorbed energy of the empty and filled conical tubes. The DAF of the empty tube initially increases and then decreases as the deflection increases. Unlike empty tube, the DAF of the filled tube shows a wavy pattern. Also, the increase in the DAF due to the increase in impact velocity varies with increasing deflection for the empty tube; while this increase is smaller for the filled tube. Furthermore, it is noteworthy that the DAF of the filled tube is higher than that of the empty tube. From Fig.7, the DAF can be as high as 44% and 47% for the empty and filled tube, respectively, for a constant impact velocity of 50 m/s.

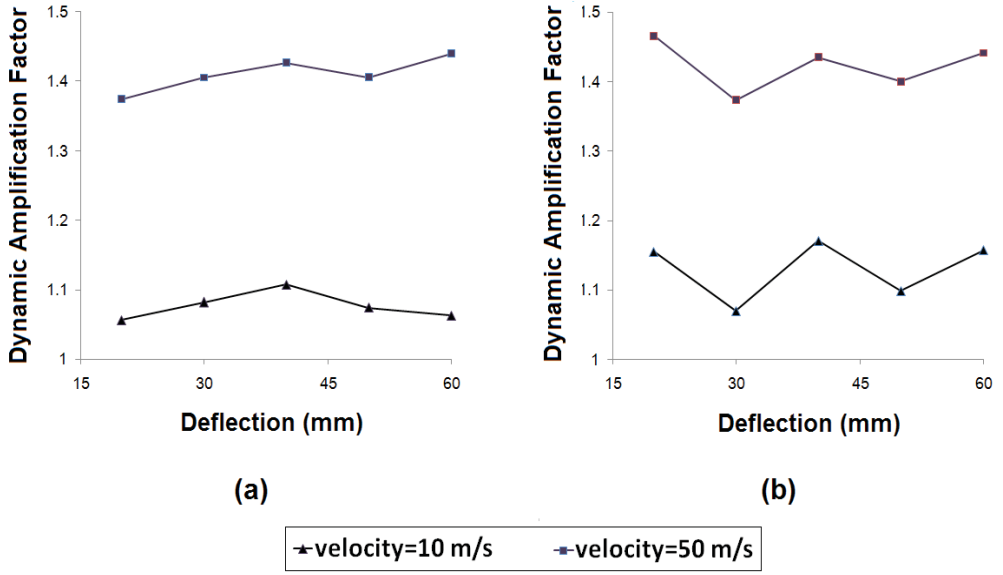


**Figure 8. The effect of impact velocity on dynamic amplification factor of (a) empty and (b) foam-filled conical tubes; (thickness=1mm, h=100 mm, semi-apical=10 deg, m=20 kg)**

### 5.2 Effect of wall thickness on the DAF

The effect of wall thickness on the DAF of absorbed energy is illustrated in Fig. 9 for a constant semi-apical angle and impact velocity of θ=10° and v=10 m/s, respectively. For the empty and filled tube, the DAF changes appreciably with the increase in wall thickness. However, the DAF of the empty tubes unlike filled tubes increases significantly with increasing wall thickness toward the start and end of the crush process. Furthermore, the DAF of filled tube for a given wall thickness and deflection is generally lower than that of an empty one.

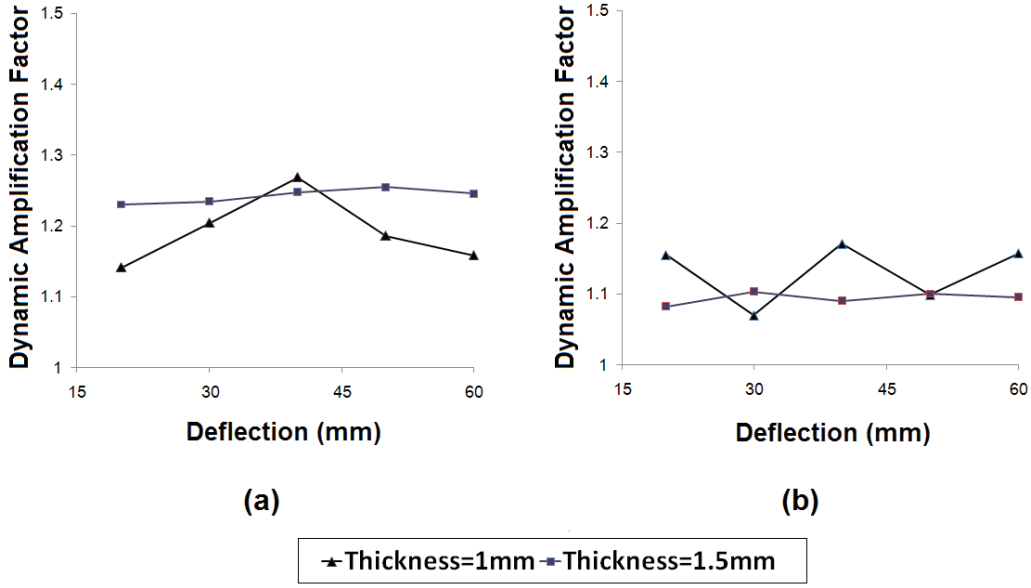


**Figure 9. Effect of wall thickness on the DAF of the absorbed energy of (a) empty and (b) foam-filled conical tubes(h=100 mm, semi-apical=10 deg, m=20 kg)**

The specific energy absorptions of the empty and foam filled tubes with different thicknesses and at different impact velocities are presented in table 6. Here, to calculate the specific energy absorptions of the tubes, the energy absorptions of the tubes at 60 mm deformations are considered. From this table it is clear that the specific energy absorptions of the tubes with the thicknesses of 1 and 1.5 mm under dynamic loading are higher than quasi-static loading.

**Table 6. Specific energy absorptions of the empty and foam filled tubes ( h=100 mm, angle=10 deg)**

| **Thickness** | **t=1mm** | | |
|---|---|---|---|
| Type of loading | Quasi-static | Dynamic (10 m/s) | Difference (%) |
| Empty | 11.83 | 12.58 | 6.34 |
| Filled (with density 145 kg/m$^3$) | 12.57 | 14.54 | 14.95 |
| **Tickness** | **t=1.5 mm** | | |
| Type of loading | Quasi-static | Dynamic (10 m/s) | Difference (%) |
| Empty | 13.37 | 14.70 | 9.94 |
| Filled (with density 145 kg/m$^3$) | 14.23 | 15.58 | 9.48 |

### 5.3 Effect of semi-apical angle on the DAF

It was also interesting to investigate the effect of semi-apical angle on the DAF of absorbed energy of the empty and filled conical end-capped tubes with h=1mm and v=10 m/s as shown in Fig. 10. In general, the DAF of each tube is reduced as the semi-apical angle increases from 5° to 10°. It is worth noting that the dynamic amplification factor of the filled tubes tends to converge as the crush progresses for a semi-apical angle of 10°. all in all, due to the variation in the semi-apical angle, the DAF can be as high as 11% to 15% for the empty and filled tubes, respectively, for an impact velocity of 10 m/s.

### 5.4 Effect of foam density on the DAF

Finally, the effect of foam density on the DAF at an impact velocity of 10 m/s is illustrated in Fig. 11. In general, it seems difficult to evaluate the effect of increasing the foam density on the DAF. No distinct trend is observed when varying the foam density with increasing deflection. However, it is obvious that the DAF is also notably influenced by the foam density, for a given deflection. It is noteworthy that at most points, the DAF of the filled tubes is higher than that of the empty one for a constant wall thickness and semi-apical angle. Here, it can be seen that when the foam density increases, the amplification of absorbed energy also augments as can be observed in Fig. 11, where the DAF of the filled tube with a foam density of 90 Kg/m3 is greater than the filled tube with a foam density of 65 Kg/m3.

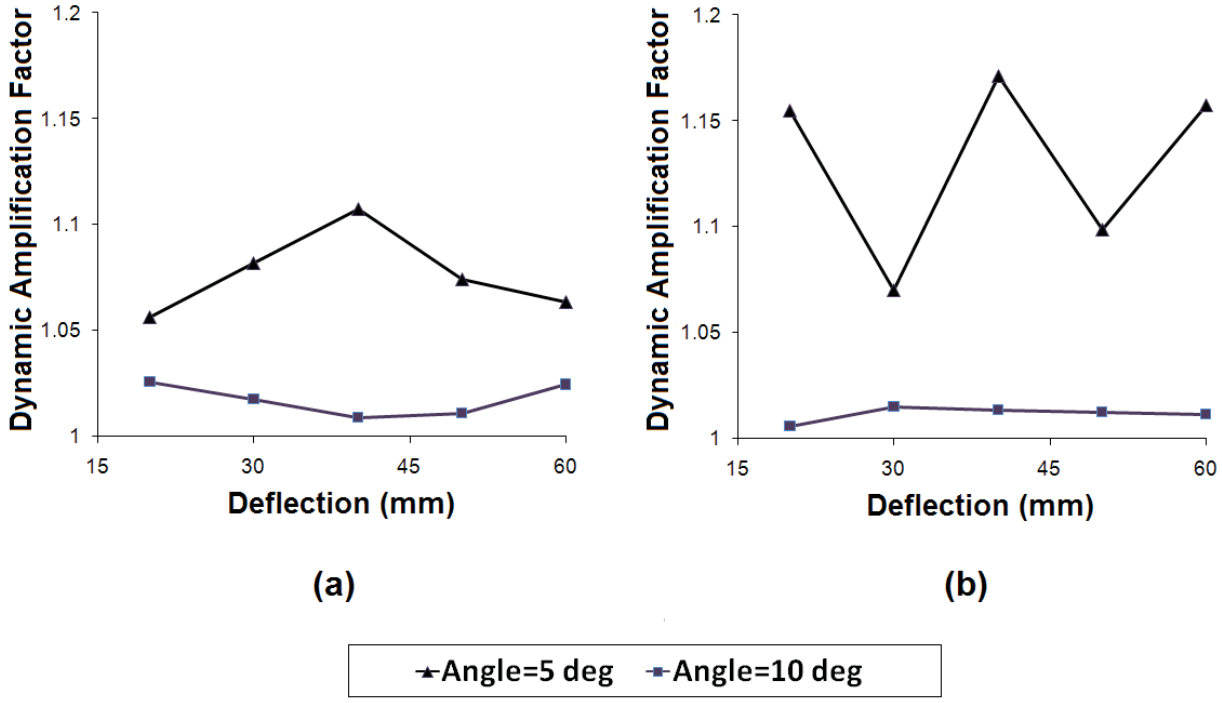


**Figure 10. Effect of semi-apical angle on the DAF of the absorbed energy of (a) empty and (b) foam-filled conical tubes(thickness= 1mm, h=100 mm, m=20 kg)**

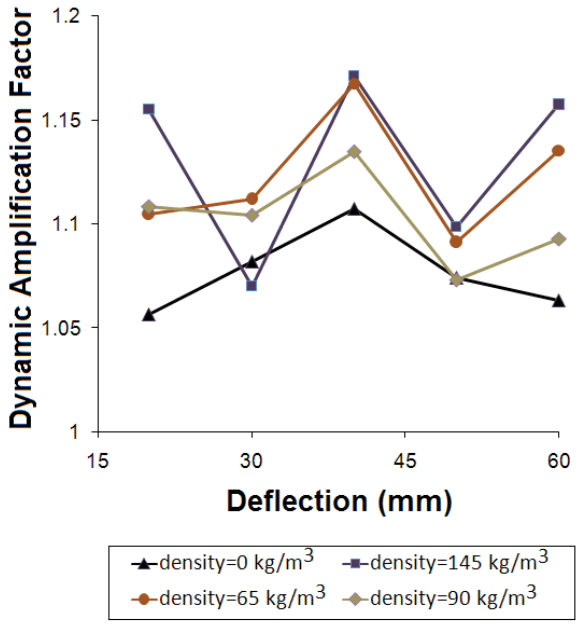


**Figure 11. Comparison of dynamic amplification factor vs. crush distance for empty and foam-filled tubes; (thickness=1mm, h=100 mm, semi-apical=10 deg, m=20 kg)**

## 6 Conclusions

A numerical simulation procedure was developed to analyze the axial crushing of empty and foam-filled end-capped conical tubes considering the nonlinear response due to large deformation, contact boundary conditions, work hardening and strain rate effects on material behavior. Based on the experimental results obtained for end-capped tubes, it was shown that the numerical method predicts the buckling and post-buckling responses with a reasonable accuracy. With the use of numerical simulations, the effects of tube parameters as well as foam density and impact velocity on the dynamic responses of the tubes were studied. The experimental and numerical studies conclude the following results:

- The presence of polyurethane foam in conical tubes has little effect on increasing the load and energy capacity and it decreases the specific energy absorption.
- The DAF of empty end-capped conical tubes is increased when the impact velocity increases; while this increase is smaller for the filled one.
- For a constant impact velocity, the DAF of the filled tube is higher than that of the empty one.
- The thickness of the tube has a considerable effect on the DAF. The DAF of the empty tubes, unlike filled tube, increases significantly with raising wall thickness towards the start and end of the crush process.
- The specific energy absorptions of the tubes with different thicknesses under dynamic loading are higher than that of the quasi-static one.
- The DAF of filled tube for a given wall thickness and deflection is generally lower than that of an empty one.
- The DAF of each tube is reduced as the semi-apical angle increases from 5° to 10°.
- The DAF of the filled tubes is higher than the DAF of empty ones for a constant wall thickness and semi-apical angle.
- The DAF of the filled tube with a foam density of 90 Kg/m3 is greater than that of the filled tube with a foam density of 65 Kg/m3.

## References

1. Wierzbicki T, Abramowizc W. On the crashing mechanics of thin-walled structures. J Appl Mech 1983; 50:727-39.
2. Abramowizc W, JonesN. Dynamic axial crashing of square tubes. Int. J. Impact Eng 1984; 2:263-81.
3. Alexander JM. An approximate analysis of the collapse of thin cylindrical shells under axial laoding. Q J. Mech.Appl Math 1960; 13:10-15.
4. Pugsley AG. On the crumpling of thin tubular structures. Q J. Mech.Appl Math 1979; 32:1-7.
5. Abramowicz W. The effective crushing distance in axially compressed thin-walled metal columns. Int. J. Impact Eng 1983; 1:309-17.
6. Abramowicz W, Jones N. Dynamic axial crushing of circular tubes. Int. J. Impact Eng 1984;2:179-281.
7. Singac AA, Elsobky H. Further experimental investigation on the eccentricity factor in the progressive crushing of tubes. Int. J. Solids Structure 1996; 32(3):589-602.
8. Wierzbiki T, Bhat SU. A moving hinge solution for axisymmetric crushing of tubes. Int. J. Mech. Sci 1986;28:135-51.

9. Zarei HR, Kr?ger M. Multiobjective crashworthiness optimization of circular aluminum tubes. Thin-Walled Structure J 2006; 44:301-8.

10. Yamazaki K and Han J, Maximization of the crushing energy absorption of tubes, Structure Optimization, 1998 16 37-49.

11. Mohamed Sheriff N, Gupta NK, Velmurugan R, Shanmugapriyan N. Optimization of thin conical frusta for impact energy absorption. Thin-Walled Structure J 2008; 46: 653-66.

12. Easwara Prasad GL, Gupta NK. An experimental study of deformation modes of domes and large-angled frusta at different rates of compression. Int. J. Impact Eng 2005; 32:400-15.

13. Gupta NK, Mohamed Sheriff N, Velmurugan R. A study on buckling of thin conical frusta under axial loads. Thin-Walled Structure J 2006; 44:986-96.

14. Gupta NK, Venkatesh R. Experimental and numerical studies of impact axial compression of thin-walled conical shells. Int. J. Impact Eng 2007; 34: 708-20.

15. Gibson L. J, Ashby M. F. Structure and Properties, 2nd, Cambridge University Press, Cambridge, 1997; 1-510.

16. Reid SR, Reddy TY. Axial crushing of foam-filled tapered sheet metal tubes. Int J Mech Sci; 1986; 28(10):643-56.

17. Zarei HR, Kroger M. Crashworthiness Optimum honeycomb filled crash absorber design. Materials & Design 2008; 29:193-204.

18. Zarei HR, Kroger M. Optimisation of the foam-filled tubes for crash box application. Thin-Walled Structure J 2008; 46, pp. 214-21.

19. Zarei HR, Kroger M. Bending behavior of empty and foam-filled beams: Structural optimization. Int. J. Impact Eng 2008; 35: 521-28.

20. Gupta NK, Velmurugan R. Axial compression of empty and foam filled composite conical shells. J Composite Materials 1999; 33(6):567-91.

21. Mirfendereski L, Salimi M, Ziaei-Rad S. Parametric study and numerical analysis of empty and foam-filled thin-walled tubes under static and dynamic loadings. Int J Mech Sci 2008; 50(6): 1042-57.

22. Ahmad Z, Thambiratnam DP. Crushing response of foam-filled conical tubes under quasi static axial loading. Materials & Design 2009; 30(7):2393-403.

23. Ahmad Z, Thambiratnam DP. Dynamic computer simulation and energy absorption of foam-filled conical tubes under axial impact loading. Computers & Structures 2009; 87(3-4):186-97.

24. A. Ghamarian, M.T Abadi, Axial crushing analysis of end-capped circular tubes. Thin-Walled Struct. 49(2011) 743-752.

25. A. Ghamarian, H.R Zarei, M.T Abadi, Experimental and numerical crashworthiness investigation of empty and foam-filled end-capped conical tubes. Thin-Walled Struct. 49 (2011) 1312-1319.

26. A. Ghamarian, H.R Zarei, Crashworthiness investigation of conical and cylindrical end-capped tubes under quasi static crash loading. Int. J. Crashworthiness 17 (2012) 19-28.

27. Gupta NK, Easwara Prasad GL, Gupta SK. Plastic collapse of metallic conical frusta of large semi-apical angles. Int J of Crashworthiness 1997; 2:349-66.

28. Abaqus user's manual. Pawtucket:Hibbitt, Karlson & Sorensen;1999

29. Aljawi A.A.N. and Alghamdi A.A.A, Abu-Mansour T.M.N, Akyurt M. Inward inversion of end-capped frusta as impact energy absorbers. Thin-Walled Structure J 2005; 43: 647-664.

30. Deshpandeh VS, Fleck NA. Multi-axial yield behavior of polymer foams. Acta materialia 2001; 49:1859-66.

31. Symonds P.S., Viscoplastic behavior in response of structures to dynamic loading, in: N.J. Huffington (Ed.), Behavior of materials under dynamic loading. New York: SME; 1965, pp. 106-24.

32. D. Karagiozova, M. Alves, N. Jones, Inertia effects in axisymmetrically deformed cylindrical shells under axial impact, Int. J. Impact Eng. 24 (2000) 1083-115.

33. M.F. Ashby, R.F. Mehl Medalist, The mechanical properties of cellular solids, Metall. Trans. A 14A (1983) 1755-69.